

# Technical Report of Resilient Subpath-Based NDN Transport Protocol for Ad-Hoc Stationary Wireless Sensor Networks

Boyang Zhou  
Zhejiang Lab  
zhouby@zhejianglab.com

## Abstract

Reliable data transport in ad-hoc stationary wireless sensor networks (WSNs) powered by sustainable energy sources is challenging due to packet losses caused by noise interference. Traditional transport protocols often neglect the role of subpaths—available routes between nodes and the sink—which are critical for enhancing resiliency. To address this, we propose RNTP, a subpath-based transport protocol leveraging named-data networking (NDN) to improve packet delivery reliability and efficiency. RNTP constructs subpaths with minimal overhead, dynamically selecting reliable routes based on channel quality and hop distance. It incorporates congestion control and fast retransmission mechanisms to optimize end-to-end performance. Simulations demonstrate that RNTP outperforms existing protocols in terms of delivery reliability, latency, and energy efficiency across various network conditions.

## 1 Introduction

Ad-hoc stationary wireless sensor networks (WSNs) play a critical role in IoT applications such as environmental monitoring, industrial automation, smart grids, and healthcare systems [1, 2, 3]. These networks, often powered by sustainable energy sources like solar panels, require reliable data transport to ensure continuous and accurate monitoring [4]. However, packet losses caused by wireless noise, interference, and congestion pose significant challenges to reliable data delivery [3].

Traditional transport protocols primarily rely on end-to-end paths, which can suffer from failures due to unpredictable channel conditions [5, 6, 7]. Subpaths, defined as partial routes between intermediate nodes and the sink, offer greater resilience by enabling dynamic rerouting and congestion avoidance. However, existing approaches fail to fully leverage subpaths, often leading to inefficiencies in packet delivery and increased energy consumption [8, 9, 10].

To address these challenges, we propose RNTP, a resilient subpath-based transport protocol leveraging Named-Data Networking (NDN) [11, 12, 13]. The source code of resilient subpath-based NDN transport protocol (RNTP) has been released online (<https://github.com/zhouby-zjl/rntp>). RNTP constructs subpaths with minimal overhead using a single reactive message propagation process. At each hop, it dynamically selects the most reliable subpath based on channel quality (CQ), considering both hop distance and signal-to-interference-plus-noise ratio (SINR) [14]. It integrates feedback-driven congestion control and fast retransmission mechanisms to improve end-to-end packet delivery and energy efficiency.

Our simulations in ndnSIM demonstrate that RNTP significantly reduces packet loss, delivery time, and energy consumption compared to existing approaches. In a 64-node topology under noise interference, RNTP achieves a 0.02% end-to-end failure rate (EEFR) and a 5.54s end-to-end delivery time

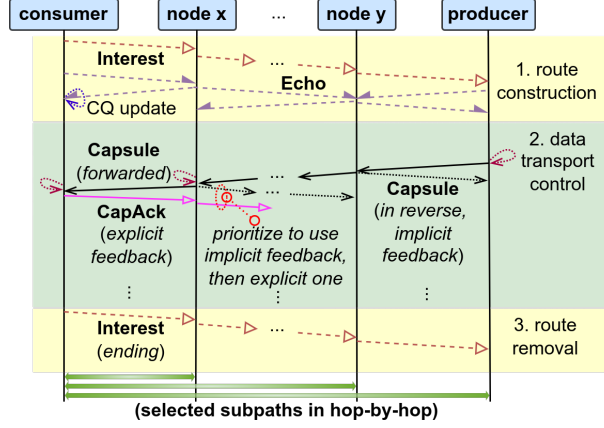


Figure 1: Overall interactions of RNTP

(EEDT), outperforming conventional protocols [15, 16]. Furthermore, experiments across WSNs with 36 to 144 nodes confirm RNTP’s scalability and robustness in dynamic, resource-constrained environments.

## 2 Protocol

Building on the consumer-driven model of NDN, the proposed RNTP enhances resilience and efficiency in ad-hoc stationary WSNs by introducing *subpaths* and a robust transport mechanism.

Fig. 1 illustrates RNTP’s interactions. A consumer requests payloads from a producer, and data is transmitted hop-by-hop along selected subpaths. Four NDN-compatible type-length-value (TLV) messages—*Interest*, *Echo*, *Capsule*, and *CapAck*—facilitate routing and transport [17].

RNTP ensures *resilient and efficient transport* through two key mechanisms:

### 2.1 Subpath Routing

RNTP enables *localized* routing by maintaining *partial paths*, which collectively form end-to-end routes. Unlike address-based approaches, RNTP embeds subpath information in messages, enabling *adaptive routing* [11].

Subpaths are categorized as:

- **Trunk subpath:** Primary route from consumer to an intermediate hop.
- **Branch subpaths:** Disjoint alternative routes from a trunk node to the producer.

Fig. 2 shows an example in an IEEE 802.11a network, where node **64** has a trunk subpath (1, 10, 19, 21, 31, 48, 64) and branch subpaths (48, 56, 64) and (48, 63, 62, 64). Disjoint branches ensure *interference-free transmission*.

RNTP prevents loops using a *path vector approach*, where *Interests* embed visited nodes. Nodes periodically send *Echos* to update channel quality (CQ) metrics, ensuring optimal subpath selection. Route expiration is managed via *ending Interests* sent by the consumer.

### 2.2 Subpath-Based Data Transport Control

RNTP employs *hop-by-hop transport control* using implicit and explicit feedback:

- **Implicit feedback:** Downstream nodes confirm reception via wireless broadcasting, reducing overhead.

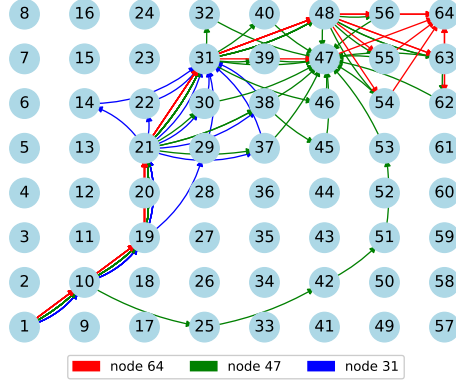


Figure 2: Example of subpath routes at various nodes in simulation [18]

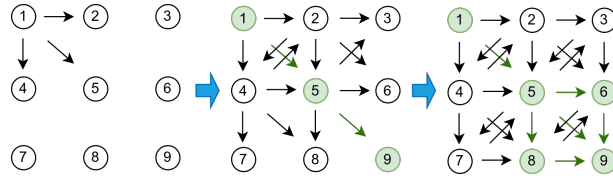


Figure 3: Subpath route construction process

- **Explicit feedback:** *CapAck* messages confirm delivery and detect duplicates.

These feedback mechanisms support:

- **Congestion control:** Nodes adjust forwarding rates based on traffic conditions.
- **Fast retransmission:** Lost packets are recovered via *alternative branch subpaths*, enhancing reliability.

By integrating *subpath routing* with *localized transport control*, RNTP enables *efficient and resilient data transport* in lossy and dynamic WSNs. The following sections detail its performance and implementation.

## 2.3 Subpath-Based Routing

To address challenge 1, RNTP integrates named-data network (NDN)'s Interest-based retrieval with subpath routing, leveraging CQ values for efficient selection.

### 2.3.1 Efficient Route Management

RNTP constructs subpath routes using NDN's Interest propagation:

- Each node broadcasts only the first received Interest to avoid loops.
- Interest trajectories are recorded with CQ metrics (e.g., signal-to-interference-plus-noise ratio (SINR)).

Fig. 3 illustrates subpath formation in a 9-node grid. The constructed paths include a trunk subpath (1, 5) and branch subpaths (5, 9), (5, 6, 9), and (5, 8, 9).

**Efficiency:** Each node forwards an Interest once, reducing overhead to  $O(n)$ . Path length scales as  $O(\max(u, v))$  in a  $u \times v$  grid and  $O(n)$  in linear topologies. Routes are removed via an ending Interest, ensuring minimal overhead.

### 2.3.2 Route Table and CQ Measurement

Each node maintains a route table  $\Upsilon = \{(\rho, \Omega_\rho)\}$ , where  $\rho$  is a subpath, and  $\Omega_\rho$  stores CQ values. The CQ metric ( $\omega_b^j$ ) is updated within a bounded time using:

$$\omega_b^j = \begin{cases} \alpha\omega_b^j + (1 - \alpha)\text{SINR} & \text{if arrival} \wedge \omega_b^j \neq \text{broken} \\ \text{SINR} & \text{if arrival} \wedge \omega_b^j = \text{broken} \\ \text{broken} & \text{if no arrival} \end{cases} \quad (1)$$

$$PIAT_{\text{est}} = \min \left( -\frac{\log(1 - \theta_{\text{piat}})}{\lambda_{\text{mean}}}, PIAT_{\text{max}} \right) \quad (2)$$

### 2.3.3 Optimized Subpath Selection

RNTP selects high-metric subpaths for reliable Capsule forwarding based on:

- *Hops*: Fewer hops reduce latency.
- *SINRs*: Higher SINRs improve reliability.

The subpath metric is computed as:

$$\text{metric}(\Omega_\rho) = \left( \prod_{2 \leq u \leq b} \omega_u \right)^{1/(2 \cdot (b-1))} \quad (3)$$

To ensure robustness,  $\text{LookupSubpath}(\Upsilon, k, \rho_{\text{prev}})$  selects candidate subpaths avoiding broken CQ values and overlapping with upstream nodes of  $\rho_{\text{prev}}$ :

$$P' = \{(\rho', \text{metric}(\Omega'_\rho)) \mid (\rho', \Omega'_\rho) \in \Upsilon \wedge \text{broken} \notin \Omega'_\rho \wedge \rho' \cap U = \emptyset\} \quad (4)$$

If  $P'$  is non-empty, the  $k'$ -th highest metric subpath is chosen ( $k' = k \bmod |P'|$ ), ensuring diverse subpath utilization and reducing congestion. This approach enables adaptive, high-quality subpath selection for resilient data transport.

## 2.4 Resilient Subpath-Based Data Transport Control

RNTP builds on the selected high-metric subpaths to enable a robust hop-by-hop transport control mechanism. This integrates path-vector-based Capsule forwarding, adaptive congestion window (CWnd) adjustment, and fast retransmissions, supported by a FIFO-based content storage (CS) for efficient retransmission. Unlike conventional approaches prone to excessive retransmissions and congestion in stationary wireless sensor networks (WSNs), RNTP mitigates end-to-end packet delivery failure rate (EEFR) and end-to-end packet delivery time (EEDT), ensuring reliable Capsule delivery under dynamic and lossy conditions.

### 2.4.1 Robust Subpath-Based Capsule Forwarding

Path-vector-embedded Capsules enhance payload delivery by improving both reliability and efficiency. Each node processes incoming Capsules based on two rules:

- If the path vector is non-empty and the next-hop CQ meets a threshold, the Capsule follows the vector.

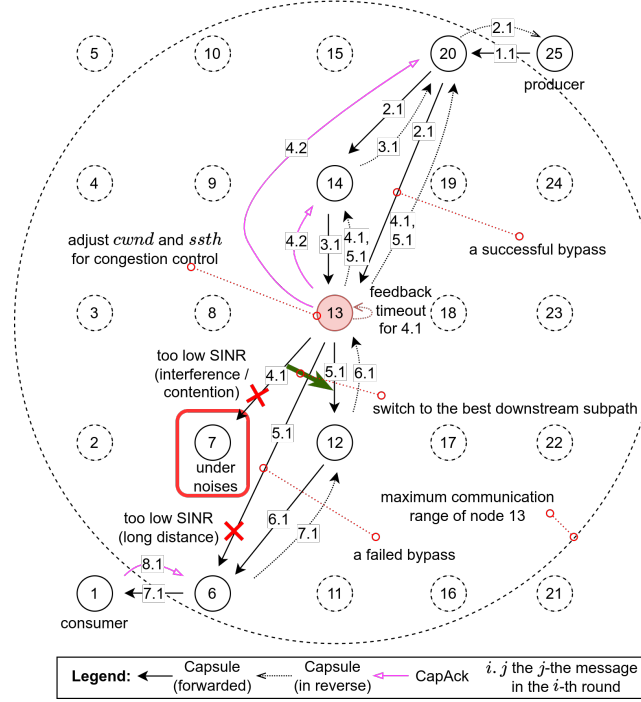


Figure 4: Capsule transport process: solid circles denote route nodes, dashed circles denote others. Labels " $i, j$ " indicate round and sequence numbers.

- Otherwise, a locally selected high-quality subpath replaces the downstream portion.

This enables two key features:

- *Efficient subpath failover*: Nodes dynamically select alternative subpaths upon failure. For instance, if node 13 detects a failure to node 7, it retrieves the Capsule from CS and reroutes via subpath 2 (12, 6, 1), ensuring uninterrupted transport.
- *Immediate node bypass*: Capsules opportunistically bypass intermediate nodes, reducing latency and hop count. For example, Capsule 2.1 from node 20 bypasses node 14 to reach node 13, provided sufficient SINR.

By combining these features, RNTP significantly improves resilience and efficiency in ad-hoc stationary WSNs.

#### 2.4.2 Resilient Transport Control

Building on subpath-based forwarding, RNTP employs a transport control policy leveraging implicit and explicit feedback to ensure reliable and efficient data delivery.

- *Implicit feedback (Capsule in downstream)*: The successful forwarding of a Capsule implicitly confirms its reception upstream, reducing message overhead. For example, node 13 accepts Capsule 2.1 from node 20 and forwards Capsule 4.1, signaling successful delivery to upstream nodes.
- *Explicit feedback (CapAck in downstream)*: Upon receiving a Capsule, the consumer or intermediate nodes send a CapAck to upstream nodes, preventing redundant retransmissions.

This policy optimizes transport via:

(i) **Congestion control**. Each node adjusts its CWnd (*cwnd*) using additive increase and multiplicative decrease (AIMD), balancing efficient utilization and congestion avoidance:

Table 1: Congestion control policy in RNTP

Event	Next Hop	Congestion Window Size ( $cwnd$ )	Slow Start Threshold ( $ssth$ )
Feedback received	Available	$\begin{cases} 2 \times cwnd, & 1 \leq cwnd < ssth \\ cwnd + 1, & cwnd \geq ssth \end{cases}$	$ssth + 1$
Feedback timeout	Broken	0	$\max(ssth/2, 1)$
	Available	$\max(cwnd/2, 1)$	
Any RNTP message arrival	Available	$cwnd_{init}$ , if $cwnd = 0$	$ssth_{init}$ , if $cwnd = 0$
Transport initialization	Available	$cwnd_{init}$	$ssth_{init}$

- When next hops are available,  $cwnd$  increases—doubling in slow start ( $1 \leq cwnd < ssth$ ) and incrementing linearly in congestion avoidance ( $cwnd \geq ssth$ ).
- When next hops fail,  $cwnd$  is halved until zero, preventing congestion.
- Upon restoration or initialization,  $cwnd$  and  $ssth$  reset to configurable initial values.

Table 1 details these rules.

(ii) **Retransmission.** Each Capsule can be retransmitted up to  $\eta_{max}$  times until valid feedback is received. Retransmission occurs upon a timeout ( $\tau_{cap}$ ) and proceeds along a high-metric subpath if available; otherwise, it is paused to avoid congestion.

Since retransmissions may cause out-of-order arrivals, the consumer temporarily buffers Capsules and triggers resequencing after a predefined timeout, ensuring in-order delivery to the application layer.

These mechanisms collectively enhance RNTP’s resilience and efficiency under dynamic network conditions (see Section 3.2).

**Summary** RNTP integrates subpath routing and hop-by-hop transport control to address challenges in NDN-based ad-hoc stationary WSNs. By leveraging NDN’s name-based routing and in-network caching, it ensures reliable and efficient data transport in challenging environments.

### 3 Performance Evaluation

The performance of RNTP was evaluated through simulations in ad-hoc stationary WSNs, comparing it with existing transport protocols.

#### 3.1 Simulation Environment

The simulation models a stationary ad-hoc WSN using ndnSIM [15] under IEEE 802.11a [19]. The network consists of 64 nodes in an  $8 \times 8$  grid (20 m spacing) with a log-distance propagation model [20] and adaptive OFDM rate of 6 Mbps [21]. Route scalability was tested across different grid sizes.

**Data Transport Schemes:** Packets (1000 B) were transmitted up to 10 pps. TCP [22], UDP [23], and routing protocols (ad hoc on-demand distance vector routing (AODV) [5], dynamic source routing (DSR) [6], destination-sequenced distance-vector routing (DSDV) [24]) were evaluated with minor adjustments:

- *TCP*: Nagle disabled, segment size 1000 B, retry limit 3, 2 MB buffer.
- *UDP*: Default settings.

Advanced protocols (data-centric ad-hoc forwarding (DAF) [12], cache-aware congestion control mechanism (RT-CaCC) [8], fast rerouting protocol (FRP) [7]) were implemented as per specifications.

**RNTP Parameters:** The source code for RNTP is available on GitHub [18] with the following key parameters:

- $\alpha = 0.1$  (SINR fluctuation),  $\nu_{\max} = 3$  (subpath establishment),  $w_{\max} = 50$  ms (Interest collision reduction).
- $\eta_{\max} = 3$  (reliable retransmissions),  $\tau_{\text{cap}} = 0.1$  s (RTT limit),  $cwnd_{\text{init}} = 64$ ,  $ssth_{\text{init}} = 128$ .
- $\tau_{\text{echo}} = 1$  s (failure detection),  $\theta_{\text{piat}} = 99.9999\%$  (PIAT estimation),  $\tau_{\text{piat}} = 3.1$  s (channel failure).

**Channel Failure Simulation:** Gaussian-distributed noise (0–30 dB, variance 5 dB) was applied to randomly selected nodes, simulating packet loss or NIC failure. Failures occurred between 5 s and 15 s, with data transmission stopping at 20 s, covering normal, failure, and recovery phases.

**Solar-Powered Simulation:** Hybrid simulations combining ndnSIM and pvlb [25] assessed RNTP under renewable energy constraints. Each node was powered by a 15 000 mAh battery and a 40 W Siemens ST40 solar module [26]. Real weather data from Hangzhou, China (2008–2017) [27] was used for long-term sustainability analysis.

## 3.2 Performance of RNTP

### 3.2.1 Data Transport

Fig. 5 illustrates variations in different performance metrics under various noise interference levels corresponding to specific number of node failures (NNs) of 5, 10, and 15. These figures are complemented with their mean and 95th percentile performance statistics summarized in Table 2. Together, they highlight RNTP’s exceptional performance, which is discussed below.

(i) **High reliability.** As shown in Fig. 5(a), EEFR remains at 0% for NN cases when noise means do not exceed 15 dB. At higher noise means, EEFR shows minimal occurrences, with maximum values reaching only 1% under serious interference.

The occasional loss of Capsules can be attributed to transient loops among divergent subpaths at the current node, causing a forwarding deadlock at downstream nodes, as illustrated in Fig. 6. For instance, consider  $\rho_1$  (A, B, C, E, H) and  $\rho_2$  (B, D, E, C, G). If Node B tries to send Capsule  $M_4$  via  $\rho_1$ , it may fail to receive a feedback within  $\eta_{\max}$  despite reaching node C. Node B then switches to  $\rho_2$  and retries sending the Capsule. However, when the Capsule reaches node C via  $\rho_2$ , node C drops it because it has already been successfully forwarded to node E. Similarly, when the Capsule reaches node E via  $\rho_1$ , Node E drops it as it has already been received by node C. This sequence halts the delivery of the Capsule. Although transient loops are rare, they can occur. Nonetheless, RNTP significantly enhances performance (see Section 3.4).

(ii) **Low delay under noises.** As illustrated in Fig. 5(b), EEDT-N increases with higher noise means. Higher noise levels can lead to channel failures in nodes, triggering subpath failovers. The failover temporarily restricts Capsule sending in the queue, increasing EEDT-Ns. However, EEDT-Ns are still significantly less than comparative schemes (see Section 3.4).

(iii) **Out-of-order Capsules and resequence.** Variations in EEDT-N depicted in Fig. 5(c) result in occasional out-of-order occurrences due to Capsule bypassing and subpath failovers. These are effectively managed by the consumer’s resequencing with an arrival timeout of 15 s, as demonstrated in Fig. 5(d), achieving 0% OOR while slightly increasing EEDT-R. Nevertheless, EEDT-R remains much lower compared to existing schemes (see Section 3.4). Fig. 5(e) illustrates the minimum arrival timeout required to achieve 0% OOR, validating our experimental choice of 15 s for consistency. Fig. 5(f) shows the queue sizes variations, with the maximum size of 150 p. These statistics indicate the resequence effectiveness.

(iv) **Efficiency message exchange.** Figs. 5(g) and 5(h) demonstrate the average message rate per second at each node measured for different message types. The CapAck ratio (shown in Table 2) ranges

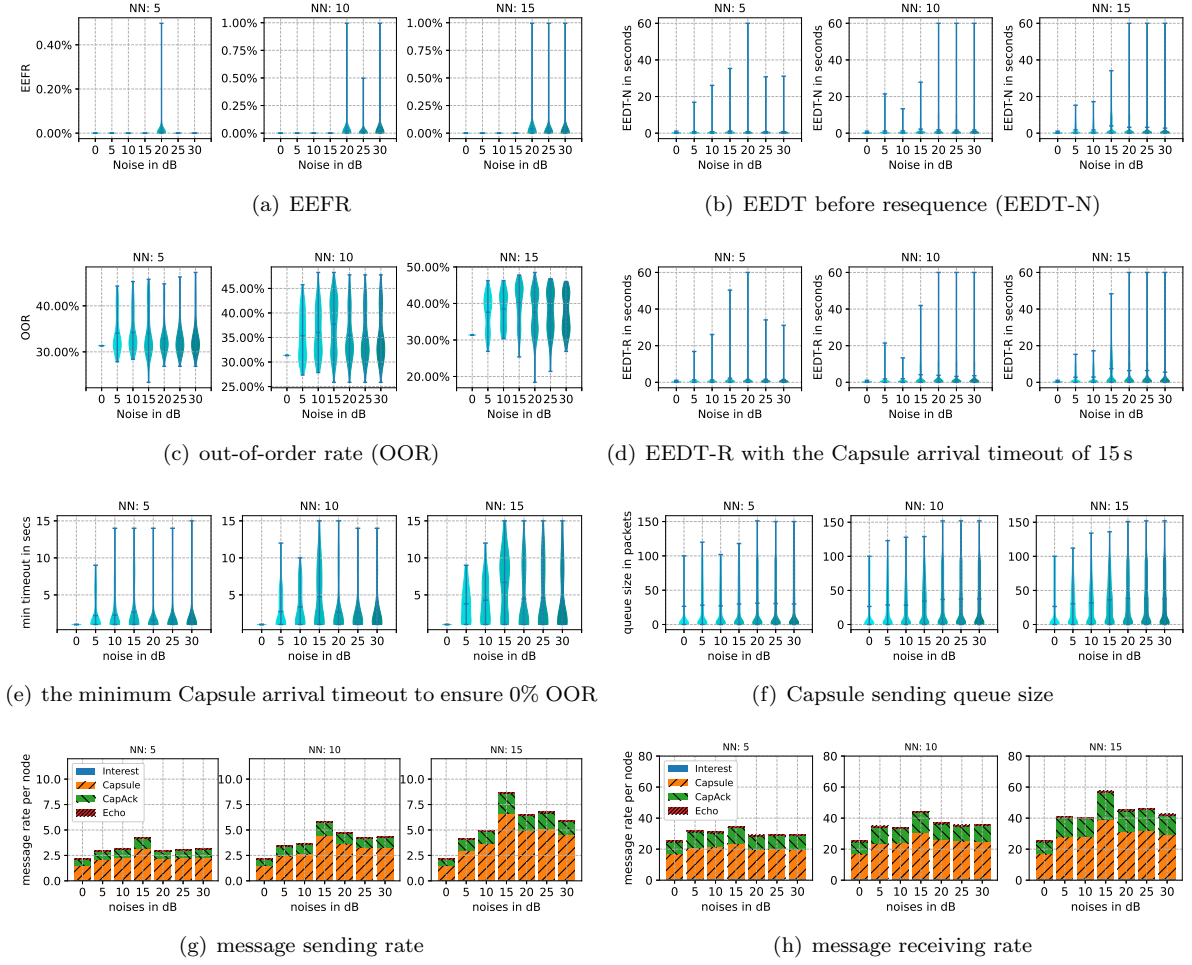


Figure 5: Performance of RNTP under various levels of noise interference for different NNs in the 64-node WSN

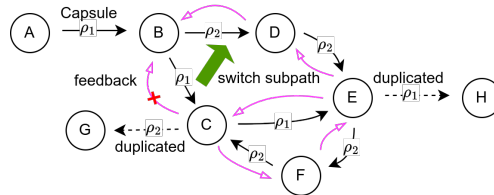


Figure 6: Capsule losses caused by transient states during a subpath failover



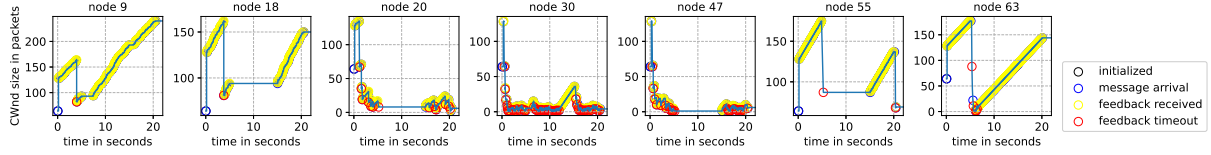


Figure 7: Congestion window changes of RNTP during data transport from node 63 to node 0 in the 64-node WSN under 30 dB noise interference for 15 NN

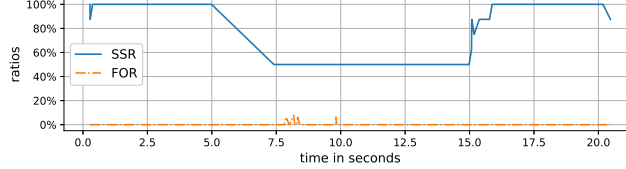


Figure 8: Corresponding subpath changes of RNTP observed at the consumer

from 29.28% to 43.26% across all test cases, reflecting the use of implicit feedback in RNTP. Additionally, the average number of Interest sending per node is 2.97 p that approximates to  $\nu_{\max}$ , indicating a subpath route complexity of  $O(n)$ . The number of received packets is magnified due to the network high density. These statistics underscore the message efficiency of RNTP.

The above statistics consistently affirm RNTP’s efficiency.

### 3.2.2 Congestion Control

Figs. 7 and 8 show the congestion control process and subpath changes of a pair, where the highest-metric path is (0, 9, 18, 20, 30, 47, 55, 63). Between 5 to 15s, 15 nodes experience 30 dB noise interference. Notably, nodes 18, 20, 47, and 55, which overlap with failure nodes, lie on the path. Fig. 7 depicts changes in CWnd annotated with corresponding events. Fig. 8 presents subpath similarity ratio (SSR) and fault overlapping ratio (FOR) for each arriving Capsule at the consumer over time.

During the period from 5s to 15s, SSR experiences fluctuations and decreases to 50%, indicating subpath adjustments to avoid channel failures. Concurrently, FOR fluctuates and eventually drops to 0%, signifying successful failover events. At the onset of the failure period, nodes 18, 20, 47, and 55 – overlapping with failure nodes – see their CWnds halve and remain unchanged until the period ends (see Fig. 7), as Capsule delivery switches to an alternative subpath involving nodes 9, 30, and 63, each exhibiting changes in CWnd. This underscores the efficacy of the congestion control process.

### 3.2.3 Subpath Route Scalability

Fig. 9(a) displays a boxplot illustrating the number of subpaths per node across different topology scales. The mean and maximum values are constrained to 13.94 and 20, respectively, both of which are less than the maximum 20 neighbors, regardless of the increase in  $n$ . This observation supports a complexity of  $O(\#\text{neighbors})$ , simplified to  $O(1)$ , as discussed in Section 2.3.

Furthermore, Fig. 9(b) shows that the mean and maximum path lengths adhere to  $O(0.35 \cdot n^{1/2} + 1.55)$  and  $O(0.9 \cdot n^{1/2} + 0.4)$ , respectively, affirming the scalability of routes.

Moreover, reroute stretches were assessed for quality across the topology scales. Fig. 9(c) shows the stretch in metric on a negative logarithmic scale, where the lowest 0 stretch is represented as -500. Fig. 9(d) shows the stretch in subpath length. Both show increased diversity with the scales due to varied subpath trajectories, but RNTP prioritizes high-metric subpaths. Despite that, the average metric stretch remains extremely low ( $10^{-398.01}$  to  $10^{-327.51}$ ). Meanwhile, the mean length stretch

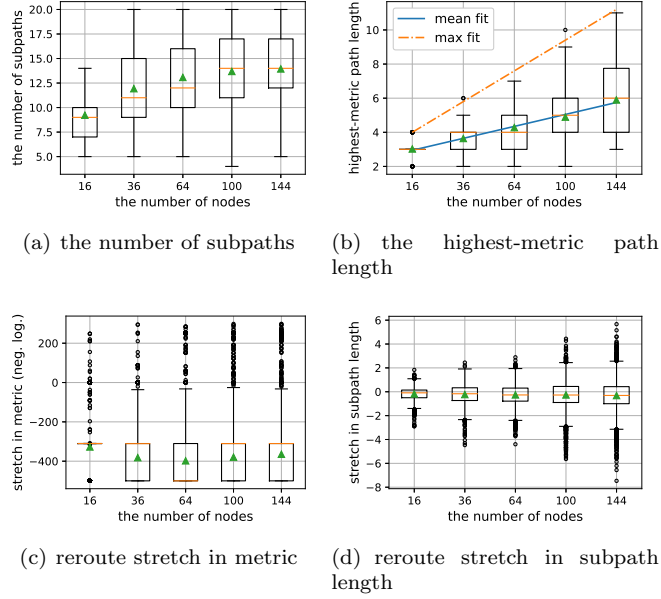


Figure 9: Subpath route quality of RNTP in the 16 to 144-node WSNs

slightly decreases from -0.18 to -0.32. These statistics consistently indicate favorable stretches of rerouted subpaths, highlighting the efficacy of the rerouting strategy.

### 3.3 Energy Consumption of RNTP

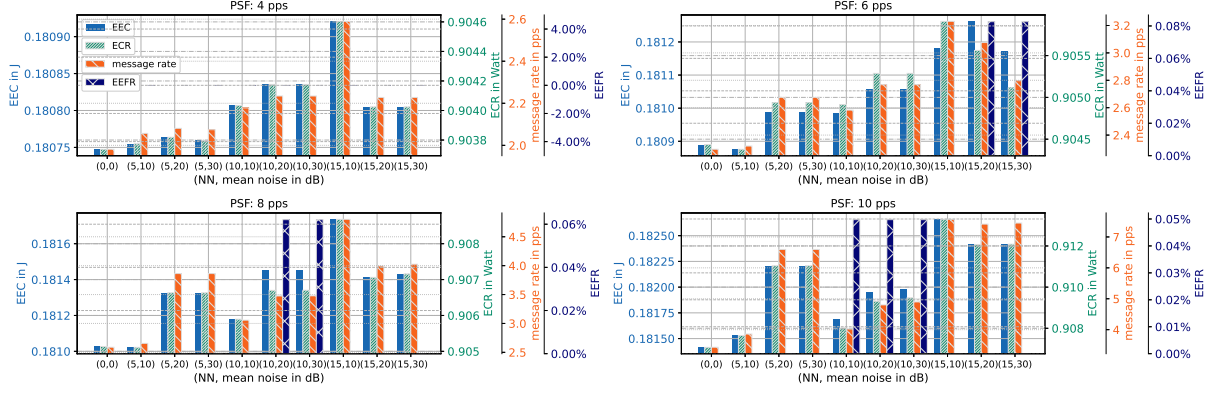
**effective energy consumption (EEC) and energy consumption rate (ECR).** Fig. 10(a) shows the relationship between the energy consumption of RNTP and its message exchange performance in the 64-node topology. The data presented include the average EEC (left y-axis) and ECR (first y-axis on the right), as well as the corresponding message sending rate per node (second y-axis on the right) and average EEFR (third y-axis on the right). The tests were under varying producer's Capsule sending frequencies (PSFs) of 4, 6, 8, and 10 pps, with channel failures characterized by NNs from 0 to 30 and mean noise levels from 0 to 40 dB.

Under all conditions, EEC and ECR exhibit minimal variations for the respective PSFs. EEC remains below  $1.73 \cdot 10^{-4}$ ,  $3.86 \cdot 10^{-4}$ ,  $7.13 \cdot 10^{-4}$ , and  $1.24 \cdot 10^{-3}$ , while ECR is limited to  $8.66 \cdot 10^{-4}$ ,  $1.53 \cdot 10^{-3}$ ,  $3.56 \cdot 10^{-3}$ , and  $6.22 \cdot 10^{-3}$ . This stability reflects the consistent message rates, which remain below 0.61, 0.93, 2.21, and 4.14 pps, respectively, as energy consumption is primarily driven by message transmissions.

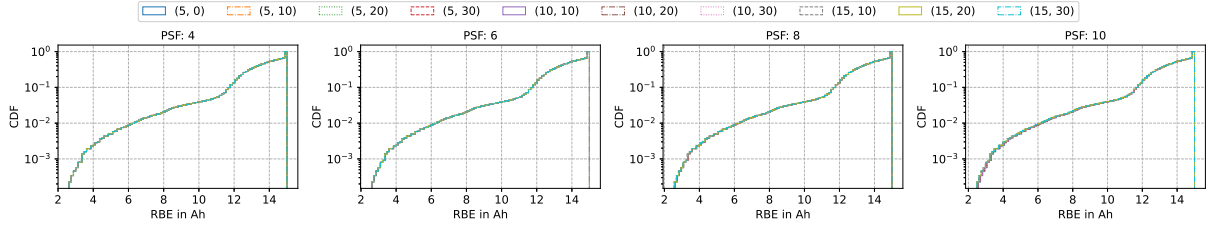
Anomalies are observed when NN reaches 15 with a mean noise level of 10 dB. In the conditions, peak values of EEC and ECR are observed, corresponding to an increased message rate. This behavior underscores the adaptability of RNTP's congestion control mechanism, which dynamically adjusts message rates to manage Capsule losses while ensuring network stability. Such adaptability shows RNTP's ability to keep energy efficiency even under challenging network conditions.

Furthermore, the variations in EEC closely mirror those in ECR, exhibiting a nearly linear relationship when the mean EEFR is close to zero. The energy consumed for retransmitting lost Capsules offsets the energy used for successful deliveries, causing an increase in EEC. In contrast, scenarios with 0% mean EEFR demonstrate a proportional relationship between EEC and ECR, reflecting both the rate and total energy consumption. These findings suggest ECR is a more appropriate metric for cross-protocol comparisons, as it offers a clearer measure of energy efficiency independent of delivery success.

**remaining battery energy (RBE).** Fig. 10(b) illustrates the CDF of RBEs (logarithmic y-axis) for the same topology. Nodes with solar-recharged batteries operate under varying PSFs and channel



(a) average EEC, ECR, and message sending rate per node, with each tick on the x axis in the format (NN, mean noise in dB)



(b) CDF of RBE across all nodes, with each legend label in the format (NN, mean noise in dB)

Figure 10: Energy performance of RNTP in a 64-node WSN under varying network loads (PSF) and conditions (NNs and noise interference levels)

failures over a 10-year simulation with a real weather dataset.

Across the above conditions, the distributions of RBEs are closely aligned due to consistent trends in ECR, despite variations in solar irradiance. The RBEs range from 2618.57 mAh to 15 000 mAh, the full battery capacity. These consistency results demonstrate RNTP's energy management efficiency, ensuring reliable performance under diverse conditions.

These results stem from RNTP's transport control mechanisms (Section 2.4.2), which dynamically select efficient subpaths and reduce unnecessary transmissions (Section 2.4.1). The mechanisms reduce the energy impact of interference and congestion, ensuring reliable and efficient operation.

### 3.4 Comparative Studies

**Statistics.** Figs. 11(a), 11(b), and 11(c) demonstrate that RNTP consistently keeps significantly lower EEFRs, EEDTs, and EECs. Its comparative schemes include RNTP, TCP-AODV, UDP-AODV, TCP-DSR, UDP-DSR, TCP-DSDV, UDP-DSDV, DAF, RT-CaCC, and FRP. RNTP achieves notable statistics for NNs (5, 10, 15) under 30 dB mean noise:

- Mean EEFRs of (0, 0.02, 0.02)%
- Mean EEDT-Ns of (0.8, 1.75, 2.75) s.
- Mean EEDT-Rs of (1.52, 3.62, 5.54) s.
- Mean EECs of (0.18, 0.19, 0.19) J.

In contrast, other schemes exhibit notably higher mean EEFRs, EEDTs, and EECs. For NN at 15 under 30 dB mean noise, their performance is characterized as follows:

- Mean EEFs of 38.77%, 27.31%, 32.68%, 22.58%, 40.59%, 42.02%, 24.88%, 74.87%, and 54.45%.
- Mean EEDTs of 24.01 s, 16.41 s, 28.78 s, 13.91 s, 26.26 s, 25.22 s, 14.94 s, 44.96 s, and 32.67 s.
- Mean EECs of 0.29, 0.25, 0.27, 0.23, 0.46, 0.47, 0.24, 0.72, and 0.4 J.

These statistics witness RNTP’s performance superiority.

**Explanation.** The superior performance of RNTP is attributed to fundamental differences in scheme designs.

The first is route establishment. TCP or UDP-based protocols (AODV, DSR, and DSDV) and NDN-based protocols (DAF and RT-CaCC) establish routes solely by hop count, often selecting unreliable paths with a low SINR or the received signal strength indication (RSSI) [14], increasing packet losses. In contrast, FRP uses a low RSSI threshold for constructing primary paths and in-path backup subpaths, relying on per-hop message flooding. This construction results in severe packet losses due to channel contention and interference, leading to frequent establishment failures. Moreover, the in-path creation method limits the backup subpath’s ability to select alternative subpaths, thereby reducing rerouting options.

The second lies in impacts of transport control policies:

- TCP’s congestion control is sensitive to packet losses, often causing a halt in payload packet transmission.
- UDP sends packets aggressively, causing packet losses.
- DAF retrieves each Data packet by having the consumer send or resend an Interest packet along an unexpired end-to-end path. This one-at-a-time retrieval method is inefficient, and reliance on unreliable paths leads to worse performance, especially under high noise conditions.
- RT-CaCC lacks effective reroute and hop-by-hop congestion control, limiting its reliability for per-hop and receiver-side retransmissions in lossy environments.
- FRP lacks effective transport control.

By fully addressing these factors mentioned, our proposed RNTP stands out as an exceptional solution. It introduces SINR-based subpath route management and tightly integrates it with hop-by-hop congestion control and fast retransmission.

## 4 Conclusion

The proposed RNTP is a robust subpath-based NDN transport protocol that enhances resiliency over existing schemes. By utilizing efficient per-hop control and a novel subpath routing structure, RNTP optimizes node trajectories and enhances rerouting options. It employs a low-complexity one-pass flooding approach for subpath route establishment and selects high-metric subpaths based on SINR and hop count for balanced payload forwarding. Congestion control and fast retransmissions are achieved through an optimized AIMD policy, significantly improving overall resiliency.

Through comprehensive simulations in stationary ad-hoc WSNs, RNTP outperforms existing protocols, showing lower EEF, EEDT-N, EEDT-R, and EEC. It also maintains efficient message exchanges and scales well with network size, achieving superior energy efficiency and stable performance under adverse conditions. These results demonstrate RNTP’s suitability for energy-constrained applications in outdoor WSNs.

We suggest further research in integrating RNTP with existing Internet of Things (IoT) platforms, extending it to mobile ad-hoc WSNs, and adapting it for real-world sensor data monitoring applications.

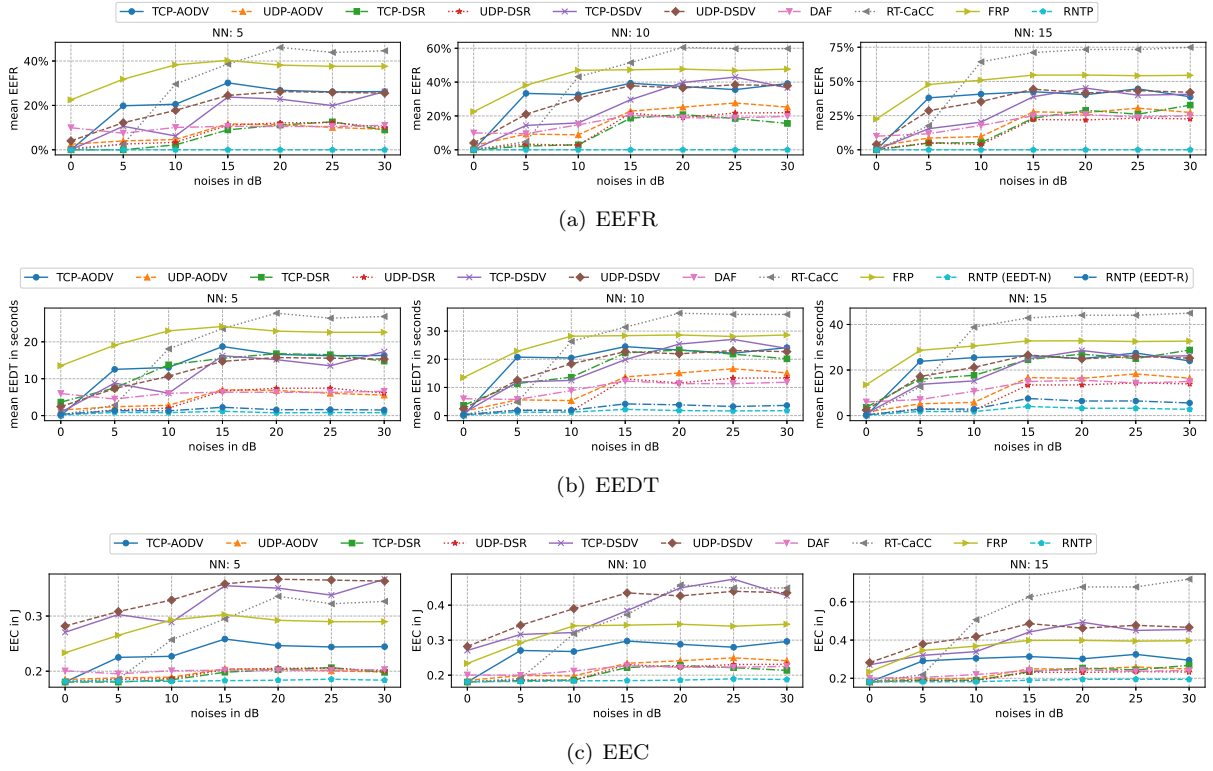


Figure 11: Performance comparison of RNTTP under various levels of noise interference for different NNs in the 64-node WSN

## References

- [1] M. A. Jamshed, K. Ali, Q. H. Abbasi, M. A. Imran, and M. Ur-Rehman, "Challenges, applications, and future of wireless sensors in Internet of things: A review," *IEEE Sensors Journal*, vol. 22, no. 6, pp. 5482–5494, 2022.
- [2] F. Wang and J. Liu, "Networked wireless sensor data collection: Issues, challenges, and approaches," *IEEE Communications Surveys & Tutorials*, vol. 13, no. 4, pp. 673–687, 2011.
- [3] M. A. Mahmood, W. K. Seah, and I. Welch, "Reliability in wireless sensor networks: A survey and challenges ahead," *Computer Networks*, vol. 79, pp. 166–187, 2015.
- [4] D. K. Sah and T. Amgoth, "Renewable energy harvesting schemes in wireless sensor networks: A survey," *Information Fusion*, vol. 63, pp. 223–247, 2020.
- [5] *Ad hoc On-Demand Distance Vector (AODV) Routing*, IETF Std. IETF 3561, 2003.
- [6] *The Dynamic Source Routing Protocol (DSR) for Mobile Ad Hoc Networks for IPv4*, IETF Std. IETF 4728, 2007.
- [7] S. Riaz, M. Rehan, T. Umer, M. K. Afzal, W. Rehan, E. U. Munir, and T. Iqbal, "FRP: A novel fast rerouting protocol with multi-link-failure recovery for mission-critical WSN," *Future Generation Computer Systems*, vol. 89, pp. 148–165, 2018.
- [8] M. I. Alipio and N. M. C. Tiglao, "RT-CaCC: A reliable transport with cache-aware congestion control protocol in wireless sensor networks," *IEEE Transactions on Wireless Communications*, vol. 17, no. 7, pp. 4607–4619, 2018.

- [9] D. N. M. Hoang, J. M. Rhee, and S. Y. Park, “Fault-tolerant ad hoc on-demand routing protocol for mobile ad hoc networks,” *IEEE Access*, vol. 10, pp. 111 337–111 350, 2022.
- [10] S. Mahajan, R. Harikrishnan, and K. Kotecha, “Adaptive routing in wireless mesh networks using hybrid reinforcement learning algorithm,” *IEEE Access*, vol. 10, pp. 107 961–107 979, 2022.
- [11] L. Zhang, A. Afanasyev, J. Burke *et al.*, “Named data networking,” *ACM SIGCOMM Computer Communications Review*, vol. 44, no. 3, pp. 66–73, 2014.
- [12] M. A. Rahman and B. Zhang, “On data-centric forwarding in mobile ad-hoc networks: Baseline design and simulation analysis,” in *IEEE ICCCN*, 2021, pp. 1–9.
- [13] F. Ansari, R. A. Rehman, and A. Arsalan, “Reduced network forwarding with controller enabled named software defined Internet of mobile things,” *Ad Hoc Networks*, vol. 149, p. 103235, 2023.
- [14] A. Goldsmith, *Wireless Communications*. Cambridge University Press, 2005.
- [15] S. Mastorakis, A. Afanasyev, and L. Zhang, “On the evolution of ndnSIM: an open-source simulator for NDN experimentation,” *ACM SIGCOMM Computer Communications Review*, vol. 47, no. 3, pp. 19–33, 2017.
- [16] A. Tariq, R. A. Rehman, and B.-S. Kim, “Forwarding strategies in NDN-based wireless networks: A survey,” *IEEE Communications Surveys & Tutorials*, vol. 22, no. 1, pp. 68–95, 2020.
- [17] (2024) NDN packet format specification. [Online]. Available: <https://named-data.net/doc/NDN-packet-spec/current/>
- [18] (2024) Resilient subpath-based NDN transport protocol. [Online]. Available: <https://github.com/zhoubu-zjl/rntp>
- [19] *IEEE Standard for Telecommunications and Information Exchange Between Systems - LAN/MAN Specific Requirements - Part 11: Wireless Medium Access Control (MAC) and physical layer (PHY) specifications: High Speed Physical Layer in the 5 GHz band*, IEEE Std. Std 802.11a, 1999.
- [20] J. Seybold, *Introduction to RF Propagation*. John Wiley & Sons, 2005.
- [21] S. Chaudhary, Ratigar, A. K. Mishra, and R. K. Singh, “Rate adaptation algorithms in IEEE 802.11 wireless networks: A comparative study,” *Journal of The Institution of Engineers (India): Series B*, vol. 104, no. 6, pp. 1369–1375, 2023.
- [22] *Transmission Control Protocol (TCP)*, IETF Std. RFC 9293, 2022.
- [23] *User Datagram Protocol*, IETF Std. RFC 768, 1980.
- [24] C. E. Perkins and P. Bhagwat, “Highly dynamic destination-sequenced distance vector (DSDV) for mobile computers,” *ACM SIGCOMM Computer Communication Review*, 1994.
- [25] A. R. Jensen, K. S. Anderson, W. F. Holmgren, M. A. Mikofski, C. W. Hansen, L. J. Boeman, and R. Loonen, “pvlib iotools—open-source python functions for seamless access to solar irradiance data,” *Solar Energy*, vol. 266, p. 112092, 2023.
- [26] (1999) Siemens solar module ST40. [Online]. Available: <https://www.siemens.co.uk/st40.pdf>
- [27] “A new solar radiation database for estimating PV performance in Europe and Africa,” *Solar Energy*, vol. 86, no. 6, pp. 1803–1815, 2012.

Table 2: Summary on performance of RNTP under various levels of noise interference for different NNs in the 64-node WSN

	(NN, noise in dB)	(0, 0)	(5, 10)	(5, 20)	(5, 30)	(10, 10)	(10, 20)	(10, 30)	(15, 10)	(15, 20)	(15, 30)
<b>mean</b>	EEFR	0%	0%	0.0%	0.0%	0%	0.02%	0.02%	0%	0.04%	0.02%
	EEDT-N	0.19 s	0.81 s	0.75 s	0.8 s	1.23 s	1.78 s	1.75 s	1.75 s	3.23 s	2.75 s
	OOR	31.34%	34.19%	32.91%	32.98%	36.02%	35.45%	35.31%	38.49%	37.62%	37.28%
	EEDT-R	0.34 s	1.29 s	1.59 s	1.52 s	1.94 s	3.81 s	3.62 s	2.9 s	6.39 s	5.54 s
	min arrival timeout	1 s	2.25 s	1.58 s	1.73 s	3.37 s	2.66 s	2.79 s	4.28 s	4.47 s	4.24 s
<b>95-p</b>	Capsule queue size	26.46 p	27.19 p	31.03 p	29.82 p	28.34 p	36.63 p	37.56 p	31.66 p	38.28 p	37.61 p
	EEFR	0%	0%	0%	0%	0%	0%	0%	0%	0.5%	0%
	EEDT-N	0.54 s	4.74 s	4.74 s	4.41 s	6.26 s	9.87 s	9.91 s	7.07 s	14.43 s	13.05 s
	OOR	31.34%	42.79%	41.82%	42.29%	43.78%	43.78%	44.22%	44.78%	45.27%	44.78%
	EEDT-R	0.83 s	6.69 s	10.51 s	9.81 s	8.3 s	19.03 s	17.76 s	9.76 s	25.43 s	23.09 s
<b>total</b>	min arrival timeout	1 s	7 s	5 s	5.25 s	8 s	10.2 s	10.1 s	9	12 s	13 s
	Capsule queue size	91 p	88 p	94 p	93 p	88 p	99 p	99 p	86 p	98 p	98 p
	msg. send rate (pps)	2.16	3.2	3.01	3.15	3.7	4.75	4.4	4.99	6.5	5.98
	msg. recv. rate (pps)	25.49	31.4	29.31	29.65	34.25	37.21	36.11	40.71	45.56	42.69
	CapAck ratio	43.26%	37.02%	36.3%	35.41%	35.65%	29.28%	31.31%	33.51%	30.53%	30.35%